Structural, Electronic and Electron Paramagnetic Resonance Study of (Pyridine-2,6-dicarboxylato)copper(II) Complexes with Substituted Imidazoles†

How Ghee Ang,[a] Whei Lu Kwik,*[,a] Graeme R. Hanson,[b] Jeffrey A. Crowther,[b] Mary McPartlin[c] and Nick Choi[c]

[a] *Department of Chemistry, National University of Singapore, Lower Kent Ridge Road, Singapore 0511, Republic of Singapore*

[b] *Centre for Magnetic Resonance and Department of Chemistry, University of Queensland, Queensland, 4072, Australia*

[c] *The Polytechnic of North London, Department of Applied Chemistry and Life Sciences, Holloway Road, London N7 8D8, UK*

The molecular and electronic structures of a series of copper(II) complexes [Cu(pydca)L][pydca = pyridine-2,6-dicarboxylate; L = imidazole, 1-, 2- or 5-methylimidazole, 2-ethylimidazole or histamine (4-aminoethylimidazole)] have been studied. The structures where L is 1- (1-mim), 2- (2-mim) or 5-methylimidazole (5-mim) have been determined by single-crystal X-ray diffraction techniques: [Cu(pydca)(1-mim)(H_2O)]·$2H_2O$, triclinic, space group $P\bar{1}$, a = 8.908(2), b = 15.729(3), c = 5.320(4) Å, α = 97.04(2), β = 91.83(2), γ = 101.64(2)°, Z = 2; [Cu(pydca)(2-mim)(H_2O)]·H_2O **2**, monoclinic, space group $P2_1/c$, a = 12.105(3), b = 13.421(3), c = 8.277(3) Å, β = 96.9(0)°, Z = 4; [Cu(pydca)-(5-mim)(H_2O)]·0.5MeOH **3**, triclinic, space group $P\bar{1}$, a = 7.575(2), b = 11.766(2), c = 16.203(3) Å, α = 69.39(3), β = 86.41(3), γ = 82.00(3)°, Z = 4, with two independent molecules in the unit cell. In each case the complex consists of discrete, monomeric units. The copper atom is co-ordinated to two carboxylate oxygen atoms [Cu–O(average) 2.0205(4), 2.0410(6) and 2.037(6) Å], to the pyridiyl nitrogen [Cu–N 1.895(4), 1.918(7) and 1.903(5) Å] and the imidazolyl nitrogen [Cu–N 1.925(4), 1.929(8) and 1.925(5) Å in **1**–**3**]. The distorted square-pyramidal geometry is completed by a longer axial bond [Cu–O 2.390(4), 2.295(5) and 2.287(6) Å] to the oxygen atom of a water molecule. The effects of the 2-methyl substituent in **2** lead to a substantially longer Cu–N(pyridyl) bond. The solid-state EPR spectra of the complexes revealed strong dipole–dipole coupling except for that with L = imidazole where antiferromagnetic exchange was involved. The frozen-glass spectra had an unusual lineshape, atypical of tetragonally or tetrahedrally distorted mononuclear copper(II) complexes. The anisotropic EPR spectra of the five-co-ordinate copper(II) complexes were fitted by an orthorhombic spin Hamiltonian from which the g and ^{63}Cu hyperfine matrices and linewidth parameters were determined by computer simulations. The methyl and ethyl derivatives of the [Cu(pydca)L(H_2O)] complexes display similarities with superoxide dismutase with respect to the EPR characteristics, *viz.* the hyperfine and linewidth anisotropy.

The unusual stability of ternary complexes of Cu^{II} containing a bidentate aromatic nitrogen base and a bidentate oxygen-donor ligand has led to extensive study of such complexes containing the chromophore CuN_2O_2.[1–5] In particular those with a α,α'-diimine as the nitrogen donor and a dicarboxylic acid as the oxygen-donor ligand have been well characterised through spectroscopic and structural studies.[6–8] In the present study, pyridine-2,6-dicarboxylic acid (or dipicolinic acid, H_2pydca) has been selected as the primary ligand acting as a dibasic tridentate ligand. Various substituted imidazoles have been selected as the second ligand so that the structural and electronic effects on the biologically important Cu–N(imidazole) bond due to the imidazole ring substituents could be probed. We report crystal structures of three of these complexes [Cu(pydca)L], *viz.* those with L = 1- (1-mim), 2- (2-mim) and 5-methylimidazole (5-mim). The electronic and EPR spectra of all six complexes of this series including those with L = imidazole (Him), 2-ethylimidazole (2-eim) and histamine (4-aminoethylimidazole) have been examined and will be discussed.

† *Supplementary data available:* see Instructions for Authors, *J. Chem. Soc., Dalton Trans.*, 1991, Issue 1, pp. xviii–xxii.

Experimental

The [Cu(pydca)L] complexes were prepared by methods similar to those reported for analogous ternary complexes.[6]

Crystal-structure Determination of [Cu(pydca)(1-mim)(H_2O)]·$2H_2O$ **1**.—*Crystal data.* $C_{11}H_{14}CuN_3O_7$, M = 363.82, triclinic, space group $P\bar{1}$, a = 8.908(2), b = 15.729(3), c = 5.320(2) Å, α = 97.04(2), β = 91.83(2), γ = 101.64(2)°, U = 732.34 $Å^3$, Z = 2, $F(000)$ = 374, D_c = 1.66 g cm^{-3}, μ(Mo-Kα) = 14.77 cm^{-1}, λ = 0.7107 Å. A blue crystal, with dimensions 0.20 × 0.16 × 0.10 mm, was used in the data collection.

Data collection and processing. Data were collected on a Philips PW1100 four-circle diffractometer using Mo-Kα radiation from a graphite monochromator. Equivalent reflections were merged to give 1936 unique reflections with $I/\sigma(I) > 3$. Absorption corrections were applied to the data

after initial refinement with isotropic thermal parameters for all atoms.

Structure solution and refinement. The coordinates of the metal atom were obtained from a Patterson synthesis and the remaining non-hydrogen atoms from a Fourier difference map. A Fourier difference synthesis calculation, with $\sin\theta < 0.35$, revealed the positions of all carbon-bonded hydrogens, and those of the water molecules, and these were included in structure-factor calculation, then thermal parameters were tied to an extra free variable which refined to 0.07 Å^2, but the coordinates were not refined. Anisotropic thermal parameters were assigned to the copper, oxygen and nitrogen atoms in the final cycles of full-matrix least-squares refinement, which converged at $R = 0.0553$ and $R' = 0.0540$ with weights of $1/\sigma^2(F)$ assigned to individual reflections. Fractional co-ordinates are given in Table 1 and selected bond lengths and angles in Table 2.

Crystal Structure Determination of [Cu(pydca)(2-mim)-(H_2O)]·H_2O **2**.—*Crystal data.* $C_{11}H_{13}CuN_3O_6$, $M = 346.8$, monoclinic, space group $P2_1/c$, $a = 12.105(3)$, $b = 13.421(3)$, $c = 8.277(3)$ Å, $\beta = 96.9(0)°$, $U = 1335.0(7)$ Å^3, $Z = 4$, $F(000) = 708$, $D_c = 1.725$ g cm^{-3}, μ(Mo-Kα) = 16.69 cm^{-1}; $\lambda = 0.710\,69$ Å. A blue crystal with dimensions 0.25 × 0.18 × 0.10 mm was used in the data collection.

Data collection and processing. Siemens R3m/v diffractometer at 296 K, ω–2θ scan mode with graphite-monochromated Mo-Kα radiation, scan range 1.3°; scan speed 5.00–30.0° min^{-1} in θ; 3085 reflections collected ($3.0 < 2\theta < 53.0°$, h, k, $\pm l$), 2784 unique (merging $R = 0.046$) after data corrected for Lorentz and polarisation effects, giving 1993 with $F > 6.0\sigma(F)$.

Structure analysis and refinement. Direct method, Full-matrix least-squares refinement with all non-hydrogen atoms anisotropic and hydrogen atoms in calculated positions. Final R and R' 0.0531 and 0.0601 respectively with the weighting scheme $w^{-1} = \sigma^2(F) + 0.0010F^2$. Computations were performed using SHELXTL PLUS [9]. Fractional coordinates are given in Table 3 and selected bond lengths and angles in Table 4.

Crystal Structure Determination of [Cu(pydca)(5-mim)-(H_2O)]·0.5MeOH **3**.—*Crystal data.* $C_{11.5}H_{13}CuN_3O_{5.5}$, $M = 331.7$, triclinic, space group $P\bar{1}$, $a = 7.575(2)$, $b = 11.766(2)$, $c = 16.203(3)$ Å, $\alpha = 69.39(3)$, $\beta = 86.41(3)°$, $\gamma = 82.00(3)°$, $Z = 4$, $F(000) = 652$, $D_c = 1.646$ g cm^{-3}, μ(Mo-Kα) = 16.61 cm^{-1}, $\lambda = 0.7107$ Å. A blue crystal with dimensions 0.20 × 0.20 × 0.35 mm was used for data collection.

Data Collection and processing. Siemens R3m/V diffractometer at 296 K, ω–2θ scan mode with graphite-monochromated Mo-Kα radiation, scan range 1.3°; scan speed 3.5–15° min^{-1} in ω; 4912 reflections collected ($0 < h < 8$, $-12 < k < 12$, $-18 < l < 18$) 4550 unique after data corrected for Lorentz and polarisation effects, giving 2779 with $F > 6.0\sigma(F)$.

Structure analysis and refinement. As for complex **2**. Final R and R' 0.0514 and 0.0655 respectively, with the weighting scheme $w^{-1} = \sigma^2(F) + 0.0043F^2$. Computations were performed using SHELXTL PLUS.[9] Fractional coordinates are given in Table 5 and selected bond lengths and angles in Table 6.

Additional material available from the Cambridge Crystallographic Data Centre comprises H-atom coordinates, thermal parameters and remaining bond lengths and angles.

EPR Measurements.—X-Band (*ca.* 9.12 GHz) EPR spectra, recorded as the first derivative of absorption, were obtained using a Bruker ER-200D spectrometer. A Bruker (VT-100) flow-through variable-temperature controller provided temperatures of 120–140 K at the sample position in the cavity. Calibrations of the microwave frequency and the magnetic field were performed with an EIP 845A microwave frequency counter and a Bruker 035M gaussmeter respectively. Acceptable signal-to-noise ratios were obtained by signal averaging the spectra on a Cleveland personal computer, using the computer program SIMOPR written by R. W. Garret.[10]

Computer simulation. Simulation of the monomeric copper(II) EPR signal (S), measured as a function of magnetic field (B) and a constant frequency (ν_c), was performed using equation (1)[9]

$$S(\nu_c,B) = C\sum_{i=1}^{2}\sum_{\theta=0}^{\pi/2}\sum_{\varphi=0}^{\pi/2}\sum_{M_I=3/2}^{3/2} a_i\overline{g_1^2} f[\nu_c - \nu_o(B),\sigma_v]\,\Delta\cos\theta\,\Delta\varphi \quad (1)$$

where the constants C and a_i involve experimental parameters and the natural abundance of the two copper isotopes (^{63}Cu and ^{65}Cu) respectively and f is the Gaussian lineshape function. Angles θ and φ are the polar angles and σ_v is the linewidth. In f, $\nu_o(B)$ is the actual difference between the energy levels and is evaluated with second-order perturbation theory.[12,13] The fundamental reason for using equation (1) is given elsewhere.[14] The powder-averaged expression for the transition probability,[15] $\overline{g_1^2}$, is defined in equation (2), l_i and l_i' are the direction

$$\overline{g_1^2} = [(L_x''L_y^* - L_x^*L_y'')^2 + (L_y''L_z^* - L_y^*L_z'')^2 + (L_z''L_x^* - L_z^*L_x'')^2]/2g^2 \quad (2)$$

where $L_i^* = \sum_{ij=x,y,z} l_i g_{ij}$ and $L_i'' = \sum_{ij=x,y,z} l_i' g_{ij}$

cosines relating the applied and microwave magnetic fields to the principal g axes (x,y,z). The angular integration was performed using the igloo method [16] which generates the angles θ and φ by holding the solid-angle segment nearly constant. The numbers of θ and φ orientations used to generate the randomly oriented spectra in this study were 50 and 30 respectively. With these values the igloo method reduced the computational time by a factor of approximately 2 when compared to using equal increments of $\Delta\cos\theta$ and $\Delta\varphi$.[16]

The linewidth σ_v as a function of the polar angles θ and φ, required for randomly oriented (frozen solution) spectral simulations, is assumed to behave in an analogous manner to hyperfine structure, *viz.* as in equation (3a).

$$\sigma_v^2 = \sum_{i=x,y,z} g_i^2 l_i^2 \sigma_i^2 \quad (3a)$$

Correlated g and A strain [17] in frequency space [14] were used to calculate the actual linewidth (σ_i, $i = x,y,z$) as a function of $\nu_o(B)$ and the nuclear spin quantum number M_I, equation (3b).

$$\sigma_i^2 = \sigma_{R_i}^2 + [C_{1_i}\nu_o(B) - C_{2_i}M_I]^2 \quad (3b)$$

The σ_{R_i} are residual linewidths, due to dipolar broadening and/or unresolved metal and ligand hyperfine interactions, while C_1 and C_2 represent strain-induced distributions of the g and A values. A unique set of linewidth parameters cannot be determined for resonances in which metal hyperfine coupling is unresolved.

In all cases spectral fits were refined using an automatic least-squares fitting program EPR50FIT [18] on the University of Queensland's Prentice Computer Centre's (PCC) IBM 3081 computer. The quality of the final simulated spectrum can be estimated from the least-squares error (l.s.e.) parameter, equation (4),[19] where I_E and I_S are normalisation factors

$$\text{l.s.e.} = \sum_{i=1}^{N} [(E_i/I_E) - (S_i/I_S)]^2/N \quad (4)$$

(doubly integrated intensities) and N is the number of points in both the simulated (S) and the experimental (E) spectra. Spectral subtractions, comparisons and the determination of l.s.e. were carried out with the EPR software package EPR PLOT [18] running on the PCC's VAX 8550 computer.

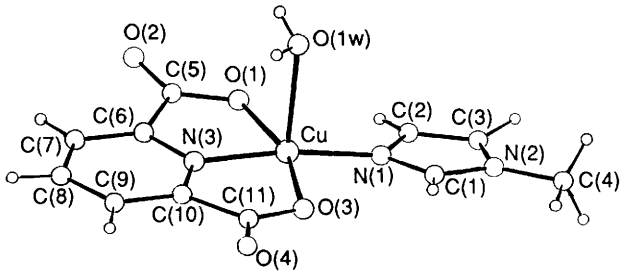

Fig. 1 Structure of the complex [Cu(pydca)(1-mim)(H_2O)] showing the atomic numbering scheme used; molecules of water of crystallisation have been omitted for clarity

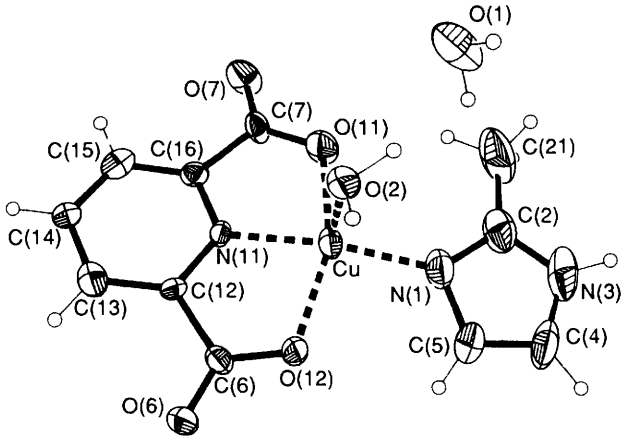

Fig. 2 Structure of the complex [Cu(pydca)(2-mim)(H_2O)] showing the atomic numbering scheme used; molecules of water of crystallisation have been omitted for clarity

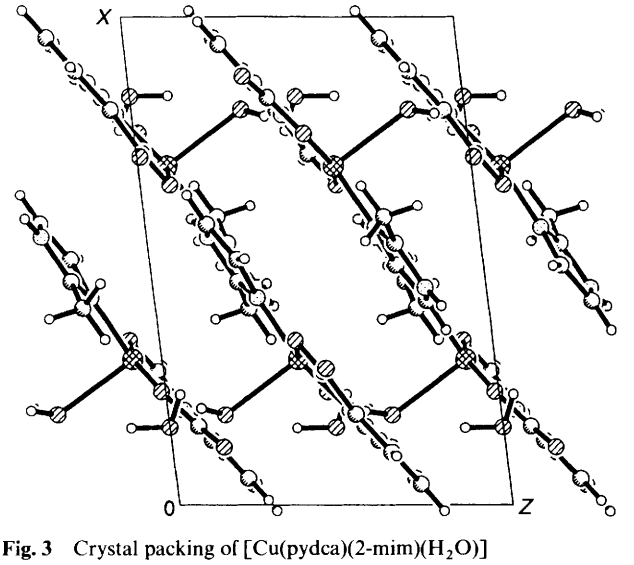

Fig. 3 Crystal packing of [Cu(pydca)(2-mim)(H_2O)]

The g and hyperfine parameters and the relative orientation of the two copper sites were determined from the EPR spectrum of a dipole–dipole coupled binuclear copper(II) complex by simulating the $\Delta M_s = \pm 1$ transitions with the Fortran program DISSIM.[20] The effect of g and A strain on the linewidths has not been taken into account in this program. Consequently, the quality of the simulations is not expected to be as high as those for mononuclear copper(II) complexes although reproduction of the resonance field positions should still be attainable.

Results and Discussion

Description of the Structures.—[Cu(pydca)(1-mim)(H_2O)]·$2H_2O$ **1**.—The crystal structure of complex **1** consists of mononuclear units in which the copper(II) ion assumes approximate square-pyramidal geometry. An oxygen atom O(1w) from a water molecule is in the apical position. Two nitrogen atoms [N(1) from 1-mim and N(3) from pydca] and two oxygen atoms [O(1) and O(3) from pydca] comprise the basal plane as shown in Fig. 1 which also gives the atomic numbering scheme. Atoms N(1), O(1), O(3) and N(3) fall on a plane, the largest deviation from the mean plane being 0.036 Å for N(3). The copper(II) ion is ≈0.10 Å above this plane. The Cu–N(3) distance [1.895(4) Å] (Table 2) is significantly shorter than that of Cu–N(1) [1.925(4) Å]. The latter is also somewhat shorter than that [1.970(5) Å] in [Cu(dien)(Him)][ClO_4]$_2$ (dien = diethylenetriamine).[21] The average copper–oxygen distance is 2.0205(40) Å which is longer than those expected for monodentate carboxylate co-ordination (1.95–1.99 Å).[22] The Cu–O(1w) distance [2.390(4) Å] is longer than those [1.964(2)–1.972(2) Å] observed for similar square-pyramidal Cu^{II}.[23] The pydca ligand is planar. The dihedral angle between the copper basal plane and the pydca plane is 4.4°.

The three oxygen atoms assigned as water molecules are separated by distances characteristic of hydrogen-bonding interaction. These were O(W1)···O(W3) 2.812, O(W3)···O(W2) 2.871, H_w(2a)···O(3) 2.81, H_w(3b)···O(3), 2.98, H_w(2a)···O(4) 2.10 and H_w(2b)···O(4) 3.00 Å. In addition the carboxylate oxygen O(2) is 2.810 Å from O(W2). The internal bonding in the two carboxylic groups is almost identical, equivalent bonds having the same lengths.

[Cu(pydca)(2-mim)(H_2O)]·H_2O **2**.—The molecular structure of complex **2** is given in Fig. 2 showing the atomic numbering scheme used. The complex consists of mononuclear [Cu(pydca)-(2-mim)(H_2O)] which form parallel layers in the unit cell (Fig. 3). The co-ordinate geometry of the copper atom can be described as approximate square pyramidal. The two carboxylate oxygen atoms O(11) and O(12), the pyridyl nitrogen N(11) and the imidazolyl nitrogen N(1) form an 'O_2N_2' distorted basal square plane (Table 4). A longer apical bond of 2.295(5) Å [Cu–O(2)] to the oxygen atom of a water molecule completes the co-ordination sphere of Cu. The Cu atom is ≈0.10 Å above the best plane through atoms O(11), O(12), N(11) and N(1). The dihedral angle between the planes through atoms Cu, N(11), O(11) and Cu, N(11), O(12) is 6.0° which indicates a small distortion of the basal atoms away from

Table 1 Fractional atomic coordinates for [Cu(pydca)(1-mim)(H_2O)]·$2H_2O$ with standard deviations in parentheses

Atom	x	y	z
Cu	0.043 00(8)	−0.250 04(4)	0.234 37(15)
O(1)	0.205 1(4)	−0.226 1(2)	−0.020 9(8)
O(2)	0.415 3(5)	−0.127 4(3)	−0.079 6(9)
O(3)	−0.091 3(4)	−0.232 3(2)	0.525 8(8)
O(4)	−0.098 3(4)	−0.139 9(3)	0.878 8(8)
O(1w)	0.216 1(4)	−0.308 2(2)	0.484 0(8)
N(1)	−0.078 1(5)	−0.360 8(3)	0.080 2(10)
N(2)	−0.243 3(5)	−0.486 3(3)	0.052 2(11)
N(3)	0.139 3(5)	−0.134 2(3)	0.371 5(9)
Ow(2)	0.614 2(5)	−0.245 4(3)	−0.071 0(12)
Ow(3)	0.522 0(6)	−0.311 5(4)	0.390 8(11)
C(1)	−0.185 3(6)	−0.409 6(4)	0.197 1(12)
C(2)	−0.065 7(7)	−0.409 8(4)	−0.150 3(13)
C(3)	−0.167 3(7)	−0.487 1(4)	−0.168 2(14)
C(4)	−0.358 3(8)	−0.558 2(5)	0.124 9(16)
C(5)	0.300 5(6)	−0.151 3(3)	0.031 4(12)
C(6)	0.258 6(6)	−0.093 4(3)	0.255 0(11)
C(7)	0.329 3(6)	−0.008 0(4)	0.347 8(13)
C(8)	0.274 8(6)	0.031 6(4)	0.562 3(13)
C(9)	0.154 4(6)	−0.013 1(4)	0.684 4(12)
C(10)	0.086 9(6)	−0.098 3(3)	0.581 4(11)
C(11)	−0.044 8(6)	−0.160 3(3)	0.672 5(12)

Table 2 Selected bond lengths (Å) and angles (°) for [Cu(pydca)(1-mim)(H_2O)]·2H_2O with standard deviations in parentheses

Cu–O(1)	2.026(4)	Cu–O(3)	2.015(4)	N(2)–C(3)	1.373(9)	N(2)–C(4)	1.464(8)
Cu–O(1w)	2.390(4)	Cu–N(1)	1.925(4)	N(3)–C(6)	1.338(7)	N(3)–C(10)	1.331(7)
Cu–N(3)	1.895(4)	O(1)–C(5)	1.299(6)	C(2)–C(3)	1.352(8)	C(6)–C(6)	1.511(8)
O(2)–C(5)	1.214(7)	O(3)–C(11)	1.279(6)	C(6)–C(7)	1.386(7)	C(7)–C(8)	1.382(9)
O(4)–C(11)	1.243(8)	N(1)–C(1)	1.322(7)	C(8)–C(9)	1.385(8)	C(9)–C(10)	1.390(7)
N(1)–C(2)	1.386(8)	N(2)–C(1)	1.346(7)	C(10)–C(11)	1.501(7)		
O(3)–Cu–O(1)	161.4(1)	O(1w)–Cu–O(1)	89.7(2)	C(10)–N(3)–C(6)	123.4(4)	N(2)–C(1)–N(1)	110.9(5)
O(1w)–Cu–O(3)	92.9(2)	N(1)–Cu–O(1)	101.4(2)	C(3)–C(2)–N(1)	109.1(6)	C(2)–C(3)–N(2)	106.5(6)
N(1)–Cu–O(3)	96.6(2)	N(1)–Cu–O(1w)	96.7(2)	O(2)–C(5)–O(1)	125.6(5)	C(6)–C(5)–O(1)	113.6(5)
N(3)–Cu–O(1)	80.9(2)	N(3)–Cu–O(3)	80.7(2)	C(6)–C(5)–O(2)	120.7(4)	C(5)–C(6)–N(3)	112.4(4)
N(3)–Cu–O(1w)	90.9(2)	N(3)–Cu–N(1)	172.1(2)	C(7)–C(6)–N(3)	119.6(5)	C(7)–C(6)–C(5)	128.1(5)
C(5)–O(1)–Cu	114.5(4)	C(11)–O(3)–Cu	114.0(3)	C(8)–C(7)–C(6)	118.2(5)	C(9)–C(8)–C(7)	121.1(5)
C(1)–N(1)–Cu	123.6(4)	C(2)–N(1)–Cu	130.2(4)	C(10)–C(9)–C(8)	118.2(6)	C(9)–C(10)–N(3)	119.5(5)
C(2)–N(1)–C(1)	105.9(4)	C(3)–N(2)–C(1)	107.5(5)	C(11)–C(10)–N(3)	111.4(4)	C(11)–C(10)–C(9)	129.1(5)
C(4)–N(2)–C(1)	126.0(6)	C(4)–N(2)–C(3)	126.3(5)	O(4)–C(11)–O(3)	125.3(5)	C(10)–C(11)–O(3)	115.1(5)
C(6)–N(3)–Cu	118.3(4)	C(10)–N(3)–Cu	118.4(3)	C(10)–C(11)–O(4)	119.5(5)		

Table 3 Atomic coordinates (× 10^4) for [Cu(pydca)(2-mim)(H_2O)]·H_2O

Atom	*x*	*y*	z
Cu	6989(1)	5219(1)	887(1)
O(2)	8125(5)	5335(4)	3308(7)
O(11)	7641(6)	3926(4)	127(8)
C(7)	8365(8)	4023(7)	−849(11)
O(7)	8794(6)	3332(4)	−1529(8)
O(12)	6605(5)	6703(4)	905(7)
C(6)	7236(7)	7262(6)	173(10)
O(6)	7171(5)	8182(4)	94(8)
N(11)	8027(6)	5741(5)	−474(8)
C(12)	8113(7)	6723(6)	−626(11)
C(13)	8906(8)	7112(7)	−1539(11)
C(14)	9567(7)	6467(7)	−2282(12)
C(15)	9445(7)	5443(7)	−2141(10)
C(16)	8654(7)	5093(6)	−1203(10)
N(1)	5726(6)	4763(6)	1900(9)
C(2)	5397(9)	3898(8)	2425(13)
C(21)	5943(11)	2935(8)	2193(16)
N(3)	4481(7)	3996(8)	3152(10)
C(4)	4214(9)	4962(10)	3141(13)
C(5)	4942(8)	5428(9)	2365(14)
O(1)	8384(7)	3511(5)	5009(9)

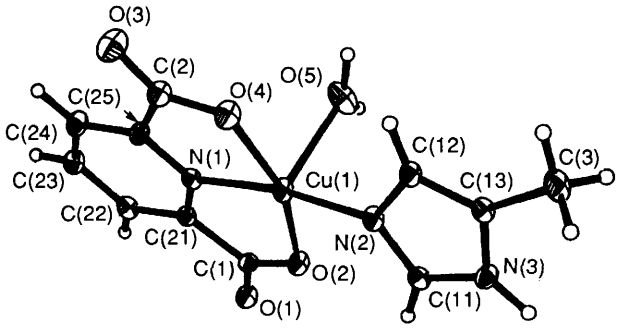

Fig. 4 Structure of the complex [Cu(pydca)(5-mim)(H_2O)] showing the atomic numbering scheme used; the molecule of methanol of crystallisation has been omitted for clarity

square planar. The pydca and 2-mim ligands are oriented such that the aromatic rings are very nearly parallel to each other with the dihedral angle between the best planes being 10.5°.

As in complex **1**, the distances of the Cu atom to the two dicarboxylate oxygen atoms [Cu–O(11) 2.037(6) and Cu–O(12) 2.045(6) Å] are longer than those expected for monodentate carboxylate co-ordination. Similarly, the copper–pyridine

Table 4 Selected bond lengths (Å) and angles (°) for [Cu(pydca)(2-mim)(H_2O)]·H_2O with standard deviations in parentheses

Cu–O(2)	2.295(5)	Cu–O(11)	2.037(6)
Cu–O(12)	2.045(6)	Cu–N(11)	1.918(7)
Cu–N(1)	1.929(8)	O(11)–C(7)	1.268(12)
C(7)–O(7)	1.232(11)	C(7)–C(16)	1.516(12)
O(12)–C(6)	1.275(11)	C(6)–O(6)	1.239(10)
C(6)–C(12)	1.502(12)	N(11)–C(12)	1.329(10)
N(11)–C(16)	1.344(11)	C(12)–C(13)	1.394(13)
C(13)–C(14)	1.374(14)	C(14)–C(15)	1.389(13)
C(15)–C(16)	1.385(12)	N(1)–C(2)	1.319(14)
N(1)–C(5)	1.390(14)	C(2)–C(21)	1.474(16)
C(2)–N(3)	1.330(15)	N(3)–C(4)	1.336(16)
C(4)–C(5)	1.311(16)		
O(2)–Cu–O(11)	96.5(2)	O(2)–Cu–O(12)	92.3(2)
O(11)–Cu–O(12)	158.2(3)	O(2)–Cu–N(11)	97.0(2)
O(11)–Cu–N(11)	79.9(3)	O(12)–Cu–N(11)	79.3(3)
O(2)–Cu–N(1)	93.7(3)	O(11)–Cu–N(1)	102.8(3)
O(12)–Cu–N(1)	96.5(3)	N(11)–Cu–N(1)	168.6(3)
Cu–O(11)–C(7)	115.6(6)	O(11)–C(7)–O(7)	125.2(8)
O(11)–C(7)–C(16)	114.4(8)	O(7)–C(7)–C(16)	120.4(8)
Cu–O(12)–C(6)	114.8(5)	O(12)–C(6)–O(6)	125.1(8)
O(12)–C(6)–C(12)	114.9(7)	O(6)–C(6)–C(12)	120.0(8)
Cu–N(11)–C(12)	118.8(6)	Cu–N(11)–C(16)	118.2(5)
C(12)–N(11)–C(16)	123.0(7)	C(6)–C(12)–N(11)	111.6(7)
C(6)–C(12)–C(13)	128.9(8)	N(11)–C(12)–C(13)	119.3(8)
C(12)–C(13)–C(14)	118.9(9)	C(13)–C(14)–C(15)	120.8(9)
C(14)–C(15)–C(16)	118.0(8)	C(7)–C(16)–N(11)	111.7(7)
C(7)–C(16)–C(15)	128.3(8)	N(11)–C(16)–C(15)	119.9(7)
Cu–N(1)–C(2)	135.2(7)	Cu–N(1)–C(5)	121.3(7)
C(2)–N(1)–C(5)	103.3(9)	N(1)–C(2)–C(21)	124.9(11)
N(1)–C(2)–N(3)	111.3(10)	C(21)–C(2)–N(3)	123.8(11)
C(2)–N(3)–C(4)	107.9(10)	N(3)–C(4)–C(5)	106.8(10)
N(1)–C(5)–C(4)	110.6(11)		

nitrogen [Cu–N(11) 1.918(7) Å] bond distance is shorter than that of the copper–imidazolyl nitrogen [Cu–N(1) 1.929(8) Å].

[Cu(pydca)(5-mim)(H_2O)]·0.5MeOH **3**. The crystal structure of complex **3** consists of discrete molecules of [Cu(pydca)-(4-mim)(H_2O)] with an interstitial methanol molecule between the two inequivalent molecules in the unit cell. The largest deviation from the mean plane of Cu, N(1), N(2), O(2), O(4) is 0.05 Å for Cu. The copper(II) ion is linked to the two carboxylate oxygen atoms O(2) and O(4) in a bidentate manner, to the pyridyl nitrogen N(1) and the imidazole nitrogen N(2). Co-ordination of an oxygen atom O(5) of a water molecule at the apical position completes an approximate square-pyramidal geometry around copper. A perspective view of **3** is depicted in Fig. 4. The two copper–oxygen distances [Cu–O(2) 2.057(6) and Cu–O(4) 2.019(5) Å] (Table 6) differ more significantly than

Table 5 Atomic coordinates ($\times 10^4$) for [Cu(pydca)(5-mim)(H_2O)]·0.5MeOH

Atom	*x*	*y*	*z*	Atom	*x*	*y*	*z*
Cu(1)	3 120(1)	3 955(1)	3 561(1)	N(1A)	1 696(7)	10 489(5)	1 661(4)
N(1)	1 736(7)	5 521(5)	3 175(4)	N(2A)	4 936(7)	7 544(5)	2 380(4)
N(2)	4 899(8)	2 540(5)	3 898(4)	N(3A)	6 402(8)	5 829(5)	3 210(4)
N(3)	6 791(8)	1 041(5)	4 688(4)	O(1A)	2 985(6)	9 313(4)	3 195(3)
O(1)	1 817(7)	5 767(4)	5 270(3)	O(2A)	1 303(6)	10 531(4)	3 812(3)
O(2)	3 049(6)	4 343(4)	4 706(3)	O(3A)	1 873(7)	10 564(5)	−519(3)
O(3)	1 647(8)	5 532(5)	1 036(4)	O(4A)	3 175(7)	9 271(4)	723(3)
O(4)	2 922(7)	4 202(4)	2 271(3)	O(5A)	5 866(7)	10 240(5)	1 654(3)
O(5)	723(7)	2 881(5)	3 972(4)	C(1A)	1 823(9)	10 223(6)	3 170(4)
C(1)	2 105(9)	5 343(6)	4 657(4)	C(2A)	2 142(9)	10 212(6)	277(5)
C(2)	1 978(10)	5 194(7)	1 818(5)	C(3A)	7 329(11)	4 690(7)	2 178(6)
C(3)	7 223(10)	−439(7)	3 878(5)	C(11A)	5 496(9)	6 910(6)	3 186(5)
C(11)	5 849(9)	2 136(6)	4 612(5)	C(12A)	5 528(10)	6 818(6)	1 880(5)
C(12)	5 258(9)	1 679(6)	3 490(5)	C(13A)	6 428(9)	5 774(6)	2 387(5)
C(13)	6 431(9)	751(6)	3 984(5)	C(21A)	1 031(9)	10 945(6)	2 282(4)
C(21)	1 291(9)	6 066(6)	3 778(4)	C(22A)	−268(11)	11 934(7)	2 051(5)
C(22)	234(9)	7 192(6)	3 531(5)	C(23A)	−850(13)	12 404(8)	1 199(6)
C(23)	−335(10)	7 723(7)	2 663(5)	C(24A)	−143(11)	11 906(7)	584(5)
C(24)	192(10)	7 138(6)	2 051(5)	C(25A)	1 168(9)	10 919(6)	834(4)
C(25)	1 254(10)	6 004(6)	2 346(5)	O	−4 411(10)	7 232(6)	−1 251(4)
Cu(1A)	3 549(1)	9 138(1)	1 979(1)	C	−4 246(20)	6 643(12)	−338(7)

those in **1** and **2**, presumably due to a lattice packing effect. The Cu–N(1) [1.903(5) Å], the Cu–N(2) [1.926(5) Å] and the Cu–O(5) (water) [2.287(6) Å] distances fall within the expected range.

The dihedral angle between the planes through Cu, O(2), O(4), N(1) and Cu, O(2), O(4), N(2) is 5.9° suggesting a distortion of the basal atoms away from square planar towards tetrahedral. The pydca ligand is nearly coplanar with these planes whereas that of 5-mim makes a substantial angle of 16°.

Comparison of Structures **1**–**3**.—A comparison of the three structures reveals several interesting features. (1) All three complexes display a co-ordination geometry approximating square pyramidal. However the constraint imposed by the pydca ligand has resulted in a distorted structure which may be described as intermediate between square pyramidal and trigonal bipyramidal with a long equatorial bond. (2) Irrespective of the substituents on the imidazole ring, the Cu–N(imidazolyl) distance remains nearly the same. The effect of the methyl substituent at the 2 position in **2** has, nevertheless, led to a considerably longer Cu–N(pydca) distance of 1.918(7) Å in the latter in comparison to 1.895(4) Å in **1** and 1.903(5) Å in **3**. The Cu–O(pydca) distances have increased somewhat from an average of 2.02(4) Å in **1** to 2.041(6) Å in **2** and 2.037(5) Å in **3**. Furthermore the apical water molecule leans closer to the 2-mim ring as the O(water)–Cu–N(imidazole) angle assumes a value of 93.7(3)° *versus* that of 96.7(2)° in **1** and 95.7(2)° in **3**. The significantly longer apical Cu–O(water) bond found in **1** is most probably due to extensive hydrogen bonding in this complex.

Electronic Spectral Study.—The solution electronic spectra in the visible region display, in each case, one broad absorption maximum in the range 715–745 nm. This band is consistent with the '4 + 1' co-ordination geometry[24,25] as shown by X-ray crystallography for [Cu(pydca)L(H_2O)] (L = 1-, 2- or 5-mim). The bands observed in the UV region at ≈324 and 294 nm are those of the ligand $\pi \longrightarrow \pi^*$ transitions as well as of ligand-to-metal charge-transfer transitions from the π-type orbitals on pydca or imidazole ring to the π*-type copper-based orbitals. The observed values of ≈324 and ≈295 nm are at higher energies compared to bands observed for a number of copper(II) imidazolates.[26,27] As the structures in solution and the solvation effects are not known, the cause of the higher energies observed for the ligand-to-metal charge-transfer (l.m.c.t.) bands of these complexes has yet to be ascertained. Moreover, it is likely that the observed bands are superposition of l.m.c.t. due to imidazole/substituted imidazole as well as to pydca. The solid-state spectra (Nujol mull) consist of one broad band centred at ≈640 nm. The shift in absorption maxima in going from solution to the solid state is consistent with increased axial interaction in solution at Cu^{II} by the rather strongly co-ordinating dimethyl sulphoxide (dmso) molecules giving rise to '4 + 2' co-ordination, in contrast to the pseudo-square-pyramidal five-co-ordinate Cu^{II} in the solid state as revealed by X-ray crystallography. As the solution spectra in dmso and methanol did not display large differences, displacement of imidazole or substituted imidazole by dmso is not likely.

Table 6 Selected bond lengths (Å) and angles (°) for [Cu(pydca)(5-mim)(H_2O)]·0.5MeOH with standard deviations in parentheses

Cu(1)–N(1)	1.903(5)	Cu(1)–N(2)	1.926(5)
Cu(1)–O(2)	2.057(6)	Cu(1)–O(4)	2.019(5)
Cu(1)–O(5)	2.287(6)	N(1)–C(21)	1.349(10)
N(1)–C(25)	1.314(9)	N(2)–C(11)	1.305(9)
N(2)–C(12)	1.381(11)	N(3)–C(11)	1.351(9)
N(3)–C(13)	1.352(11)	O(1)–C(1)	1.255(10)
O(2)–C(1)	1.269(8)	O(3)–C(2)	1.217(10)
O(4)–C(2)	1.282(8)	C(1)–C(21)	1.497(9)
C(2)–C(25)	1.521(12)	C(3)–C(13)	1.507(11)
C(12)–C(13)	1.352(8)	C(21)–C(22)	1.388(9)
C(22)–C(23)	1.391(10)	C(23)–C(24)	1.403(12)
C(24)–C(25)	1.398(9)		
N(1)–Cu(1)–N(2)	169.3(3)	N(1)–Cu(1)–O(2)	80.5(2)
N(2)–Cu(1)–O(2)	98.2(2)	N(1)–Cu(1)–O(4)	80.4(2)
N(2)–Cu(1)–O(4)	99.5(2)	O(2)–Cu(1)–O(4)	160.1(2)
N(1)–Cu(1)–O(5)	95.1(2)	N(2)–Cu(1)–O(5)	95.7(2)
O(2)–Cu(1)–O(5)	93.4(2)	O(4)–Cu(1)–O(5)	93.8(2)
Cu(1)–N(1)–C(21)	117.6(4)	Cu(1)–N(1)–C(25)	118.7(5)
C(21)–N(1)–C(25)	123.8(6)	Cu(1)–N(2)–C(11)	126.4(6)
Cu(1)–N(2)–C(12)	126.5(5)	C(11)–N(2)–C(12)	106.7(6)
C(11)–N(3)–C(13)	108.1(6)	Cu(1)–O(2)–C(1)	113.7(4)
Cu(1)–O(4)–C(2)	115.0(5)	O(1)–C(1)–O(2)	125.9(6)
O(1)–C(1)–C(21)	118.5(6)	O(2)–C(1)–C(21)	115.7(7)
O(3)–C(2)–O(4)	126.9(8)	O(3)–C(2)–C(25)	119.3(6)
O(4)–C(2)–C(25)	113.8(6)	N(2)–C(11)–N(3)	110.1(7)
N(2)–C(12)–C(13)	108.7(7)	N(3)–C(13)–C(3)	121.9(6)
N(3)–C(13)–C(12)	106.4(7)	C(3)–C(13)–C(12)	131.6(8)
N(1)–C(21)–C(1)	112.4(5)	N(1)–C(21)–C(22)	119.3(6)
C(1)–C(21)–C(22)	128.3(7)	C(21)–C(22)–C(23)	118.7(8)
C(22)–C(23)–C(24)	120.2(6)	C(23)–C(24)–C(25)	118.2(6)
N(1)–C(25)–C(2)	112.1(6)	N(1)–C(25)–C(24)	119.8(7)
C(2)–C(25)–C(24)	128.1(6)	N(1A)–Cu(1A)–N(2A)	166.0(2)

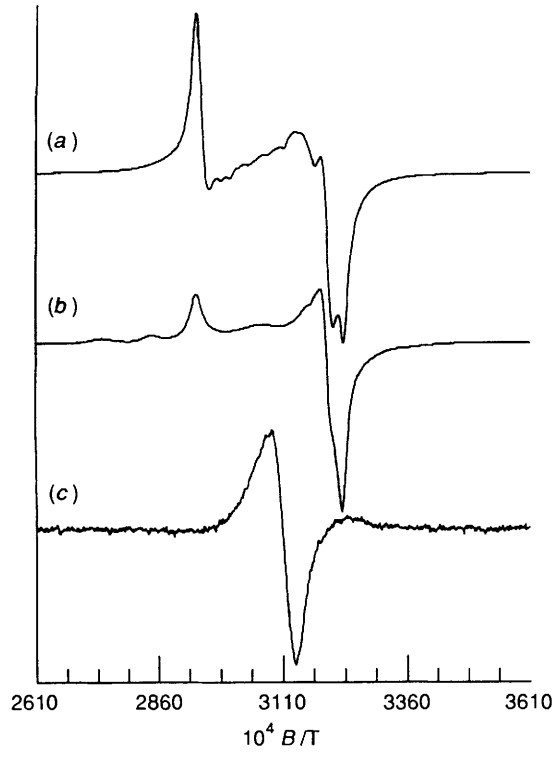

Fig. 5 EPR spectra of [Cu(pydca)(Him)]: (*a*) in the solid state, 110 K, ν = 9.2487 GHz, (*b*), (*c*) in methanol at 120 K, ν = 9.2405 GHz and 298 K, ν = 9.2556 GHz respectively

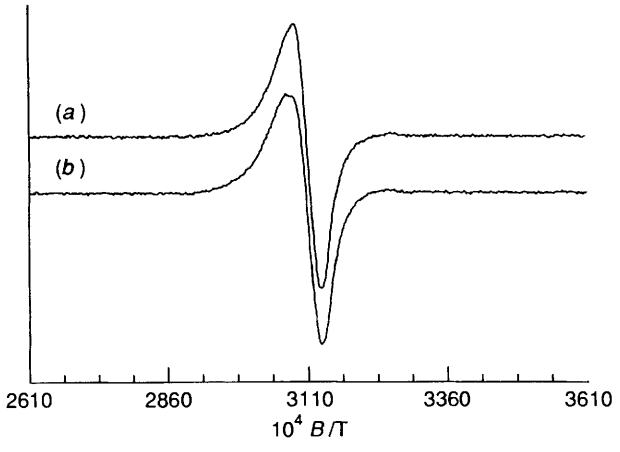

Fig. 6 Isotropic EPR spectra of (*a*) [Cu(pydca)(5-mim)(H_2O)] in methanol at 298 K, ν = 9.2462 GHz, and (*b*) [Cu(pydca)(1-mim)(H_2O)] in methanol at 298 K, ν = 9.2563 GHz

EPR Spectroscopic Study.—The solid-state and frozen-solution EPR spectra of [Cu(pydca)(Him)] [Fig. 5(*a*) and 5(*b*), Table 7] are vastly different from those of either tetragonally or tetrahedrally distorted copper(II) ($S = \frac{1}{2}$) complexes. Interestingly, the predominant EPR signal in the frozen-solution spectrum [Fig. 5(*b*)] is very similar to that observed for dichlorobis(pyridine)copper(II) [$Cu(py)_2Cl_2$] ($g_z = 2.2175$, $g_x = 2.0842$, $g_y = 2.0603$) and diaquabis(2,6-dihydroxybenzoato)copper(II)[29] ($g_{\|} = 2.335$, $g_{\perp} = 2.082$), indicating that these compounds have similar structures.

The X-ray structure of [$Cu(py)_2Cl_2$][30] reveals two linear chains per unit cell consisting of a series of stacked rhombi aligned along the *c* axis. Each rhombus consists of a central copper ion with each of the pairs of chlorine and pyridine ligands at positions *trans* to its like neighbour. The orthorhombic symmetry at the Cu arises from the arrangement of two rhombus chlorines (2.28 Å), two rhombus pyridine

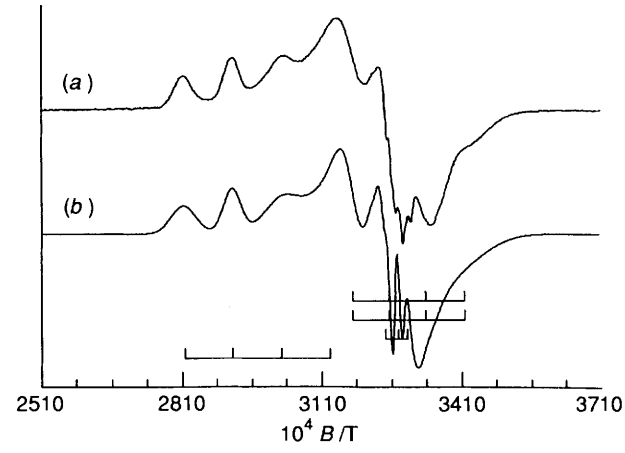

Fig. 7 EPR spectra of [Cu(pydca)(5-mim)(H_2O)] in methanol: (*a*) Anisotropic spectrum at 120 K, ν = 9.4696 GHz and (*b*) computer simulation of (*a*) with l.s.e. = 8.766×10^{-3}

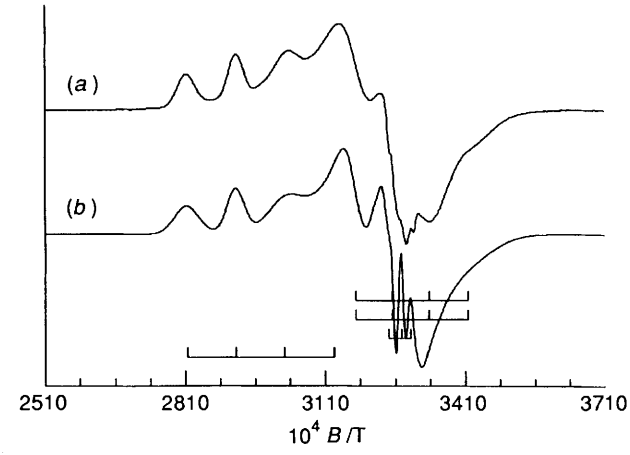

Fig. 8 EPR spectra of [Cu(pydca)(1-mim)(H_2O)] in methanol: (*a*) Anisotropic spectrum at 120 K, ν = 9.4695 GHz, and (*b*) computer simulation of (*a*) with l.s.e. = 9.725×10^{-3}

nitrogens (2.02 Å) and two next-nearest-neighbour chlorines (3.05 Å).

A thorough investigation of the magnetic and thermal properties of [$Cu(py)_2Cl_2$] by Duffy and co-workers[31,32] has established this to be a spin $\frac{1}{2}$ Heisenberg antiferromagnetic linear-chain salt in which intrachain exchange predominates over interchain exchange. A description of antiferromagnetic exchange in these types of systems can be found elsewhere.[33] Although the X-ray structure of [Cu(pydca)(Him)] is not known, the similarity of the EPR spectra indicates a linear-chain structure in which the copper ions are antiferromagnetically coupled and the symmetry around each copper(II) ion is at most orthorhombic. A comparison of the *g* values for [Cu(pydca)(Him)] with those for [$Cu(py)_2Cl_2$] shows that the former complex has a larger rhombic distortion.

Substitution of the imidazole ring at positions 1, 2 and 5 by a methyl group or at position 2 by an ethyl or position 4 by an ethylamine produces copper(II) complexes which have a distinctly different magnetic behaviour to the parent compound. Thus, the solid (powder)-state EPR spectra of these complexes revealed strong dipole–dipole coupling in contrast to the antiferromagnetic exchange found in the parent compound. Magnetic dilution was obtained by preparing 1 mmol dm^{-3} methanolic solutions of the appropriate complex. The isotropic EPR spectra of the methyl- and ethyl-substituted imidazole [Cu(pydca)L(H_2O)] complexes (Fig. 6) show a single asymmetric resonance arising from the overlap of either

Table 7 Spin-Hamiltonian parameters for the [Cu(pydca)L] complexes and superoxide dismutase

Complex[a]	g_1	g_2	g_3	A_1[b,c]	A_2[c]	A_3	g_{iso}[d]	A_{iso}[d]
[Cy(pydca)(Him)]	2.2495	2.0640	2.0458	—	—	—	2.1198	—
[Cu(pydca)(1-mim)(H_2O)][e]	2.2742	2.0668	2.0507	−111.43	−14.99	+76.60	2.1306	−16.61
[Cu(pydca)(2-mim)(H_2O)][e]	2.2873	2.0675	2.0868	−100.25	−14.56	+57.17	2.1472	−19.21
[Cu(pydca)(5-mim)(H_2O)][e]	2.2752	2.0668	2.0507	−110.84	−14.99	+76.60	2.1309	−16.41
[Cu(pydca)(2-eim)(H_2O)][e]	2.2832	2.0667	2.0582	−106.22	−14.99	+73.04	2.1360	−16.06
[Cu_2(pydca)$_2$(4-aeim)$_2$][e,f]								
Site 1	2.270	2.015	2.015	85	17	17	—	—
Site 2	2.270	2.015	2.015	85	17	17	—	—
Superoxide dismutase[g]	2.265	2.108	2.023	−140	—	—	2.132	—

[a] Isotropic and anisotropic spectra were measured at 298 and 110 K respectively in methanol. [b] Units of hyperfine coupling constants are $\times 10^{-4}$ cm^{-1}. [c] Although the absolute determination of the signs of the hyperfine coupling constants can only be achieved with circularly polarised radiation, A_1 and A_2 are assumed to be negative (see text for further discussion). [d] The isotropic g and A values were calculated from $g_{iso} = \frac{1}{3}(g_x + g_y + g_z)$ and $A_{iso} = \frac{1}{3}(A_x + A_y + A_z)$ respectively. [e] The l.s.e. values for the anisotropic computer simulations of the 1-, 2-, 5-Me, 2-Et and 4-$NH_2CH_2CH_2$ derivatives are 9.725×10^{-3}, 1.923×10^{-2}, 8.766×10^{-3}, 1.453×10^{-2} and 1.514×10^{-2} respectively. [f] The two copper(II) ions are separated by 6.85 Å with an angle of 35° between g_1 and the vector interconnecting the two copper(II) ions. [g] Ref. 28.

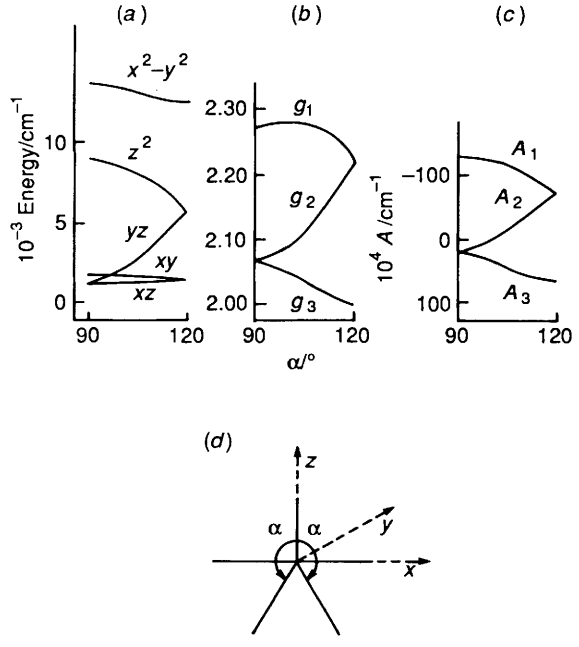

Fig. 9 (*a*) The energy-level diagram for a five-co-ordinate complex with C_{2v} symmetry as a function of the angle α. (*b*), (*c*) The dependences of the anisotropic g and A values on the angle α. (*d*) The co-ordinate system used to define the trigonal-pyramidal geometry and the angle α (reproduced from ref. 33)

copper (^{63}Cu and ^{65}Cu) hyperfine resonances. Upon freezing the solution, the EPR spectra of these derivatives were found to have an unusual lineshape atypical of tetragonally or tetrahedrally distorted mononuclear copper(II) complexes. Spin-concentration measurements[34,*] were undertaken in order to identify the number of unpaired electrons giving rise to this unusual spectrum. For the 5-methyl derivative the value of the electron spin S determined from these measurements was 0.45 indicating that a mononuclear copper(II) complex with a single unpaired electron was responsible for the EPR spectrum.

The anisotropic EPR spectra of the five-co-ordinate copper(II) complex (Figs. 7 and 8) can be described by an orthorhombic spin Hamiltonian (5). The computer-simulated g

$$\mathcal{H} = \sum_{i=x,y,z} \beta g_i B_i S_i + S_i A_i I_i \qquad (5)$$

and ^{63}Cu hyperfine matrices and linewidth parameters are listed in Tables 7 and 8. As reflected in the l.s.e. values in Table 7, the large linewidth anisotropy in the 0.313–0.341 mT region has resulted in some difficulties in reproducing the spectral features. The relative signs of the anisotropic hyperfine coupling constants were determined by a comparison of A_{iso} calculated from the trace of the A matrix (*i.e.* $A_{iso} = \frac{1}{3}(A_x + A_y + A_z)$ with that obtained from the isotropic spectrum, estimated from the linewidth at half height.

A close examination of the g and A matrices for the methyl and ethyl derivatives reveals that these complexes are characterised by strong rhombic distortions. The X-ray crystal structures of the 1-, 2- and 5-methyl derivatives indicates the copper(II) ion, in each case, is five-co-ordinated with a geometry which can be described as intermediate between a square pyramid and a trigonal bipyramid. On the basis of the angular-overlap model (a.o.m.) calculations, Bencini *et al.*[35] determined the variations in energy levels and g and A anisotropy as the geometry changes from square pyramidal to trigonal bipyramidal. The change in geometry is measured as a function of α, the angle between the Cu–N(Him) and Cu–O(pydca) bonds in the equatorial plane (Fig. 8). The copper ion's C_{2v} symmetry is maintained during the entire geometrical transformation. Calculation of the angle α from the hyperfine coupling constants for these complexes yields values in the range 106–109°, which are about 7–10° higher than those observed from crystallography (Tables 2, 4 and 6). In addition, a plot of the g values in Fig. 9(*b*) does not yield a unique solution for the angle α. These discrepancies may be a consequence of our inability to reproduce the precise spectral lineshape around the 0.313–0.341 mT region or the a.o.m. parameters used to generate the variation of the g and A values and energy levels with the angle α may not be appropriate for these complexes. In an attempt to resolve this discrepancy, a multifrequency (Q-, X-and S-band) EPR investigation of the ^{63}Cu-enriched complexes is being undertaken. The greater g-value resolution and reduced g strain at Q- and S-band frequencies respectively will lead to a more precise determination of the g and A matrices. Inclusion of at least one non-coincident angle may be required in the analysis of these spectra. Nevertheless the values of α obtained from the former plot indicate a $|xz\rangle$ ground state for these C_{2v} symmetric copper(II) complexes with g_z and A_z directed along the Cu–O(water) bond.

A re-examination of the EPR spectrum of the [Cu(pydca)(Him)] complex reveals that the minor component can be

* A double cavity operating in the TE_{104} mode was employed for these measurements using frozen solutions of copper(II) chloride as a standard. The concentration of copper(II) ions in both the standard and unknown solutions was determined by atomic absorption spectroscopy.

Table 8 Linewidth parameters for the mononuclear [Cu(pydca)L] complexes

Complex	σ_1*	σ_2	σ_3	C_{11}	C_{12}	C_{13}	C_{21}*	C_{22}	C_{23}
[Cu(pydca)(1-mim)(H_2O)]	55.74	16.49	56.99	0.0055	0.0003	0.0091	238.72	11.08	131.77
[Cu(pydca)(2-mim)(H_2O)]	49.65	22.29	34.63	0.0055	0.0003	0.0091	256.10	5.29	17.26
[Cu(pydca)(5-mim)(H_2O)]	55.76	16.49	56.99	0.0055	0.0003	0.0091	238.83	11.08	131.77
[Cu(pydca)(2-eim)(H_2O)]	55.96	19.39	25.51	0.0055	0.0003	0.0091	239.67	5.29	17.02

* Units for σ_R and C_2 are MHz.

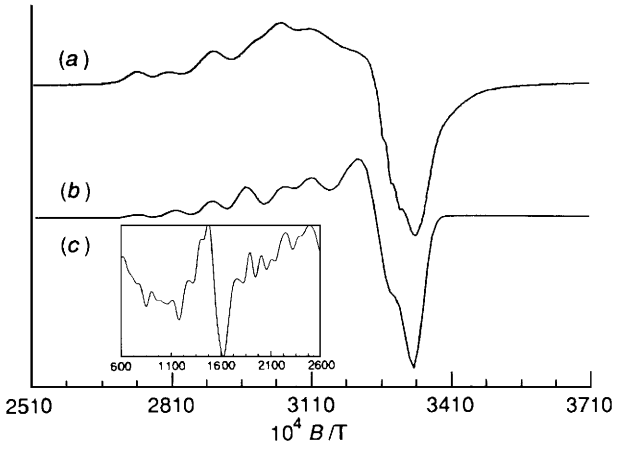

Fig. 10 EPR spectra of [Cu(pydca)(4-aeim)(H_2O)] in methanol: (*a*) anisotropic spectrum at 120 K, ν = 9.246 96 GHz; (*b*) computer simulation with l.s.e. = 1.514 × 10^{-2}; and (*c*) a Fourier-smoothed spectrum showing the $\Delta M_s = \pm 2$ transition

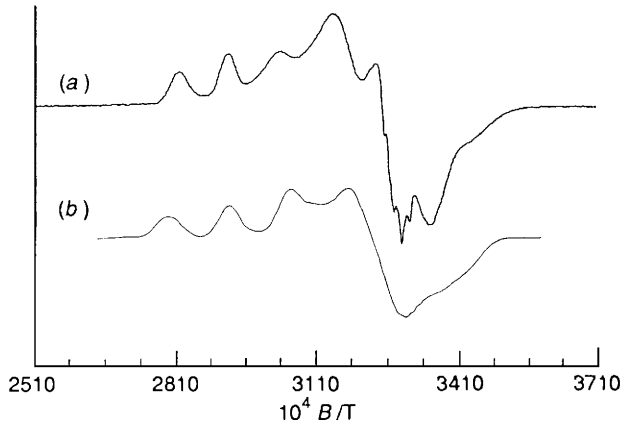

Fig. 11 A spectral comparison of the X-band EPR spectra of (*a*) [Cu(pydca)(5-mim)(H_2O)] and of (*b*) superoxide dismutase

attributed to a mononuclear copper(II) complex arising from the breakdown of the linear chain. The spectral characteristics of this signal are similar to the EPR signals obtained from the methyl- and ethyl-substituted imidazole copper(II) complexes.

The frozen-solution EPR spectrum of the histamine derivative indicates the presence of $\Delta M_s = \pm 1$ and ± 2 transitions [Fig. 10(*a*) and 10(*c*)]. Attempts at simulating the $\Delta M_s = \pm 1$ transitions with an $S = \frac{1}{2}$ spin Hamiltonian were unsuccessful suggesting that the binuclear species giving rise to the $\Delta M_s = \pm 2$ transitions was also responsible for the $\Delta M_s = \pm 1$ transitions. The dipole–dipole coupled EPR spectrum can be described by the spin Hamiltonian[20] (6) where μ_1 and μ_2 are magnetic moments of the two interacting copper(II) ions and r is the internuclear distance between them. Computer simul-

$$\mathcal{H} = \frac{\mu_1\mu_2}{r^3} - \frac{3(\mu_1 r)(\mu_2 r)}{r^5} \qquad (6)$$

ation of the experimental spectrum [Fig. 10(*b*)] was used to determine the g and ^{63}Cu hyperfine matrices of the two sites and their relative orientation (Table 7). The absence of exchange coupling indicates that the unpaired electron on each copper(II) ion is in a $|xz\rangle$ ground state (assuming a C_{2v} symmetry). A pictorial representation of the structure of the binuclear copper(II) complex [Cu_2(pydca)$_2$(4-aeim)$_2$] is shown below.

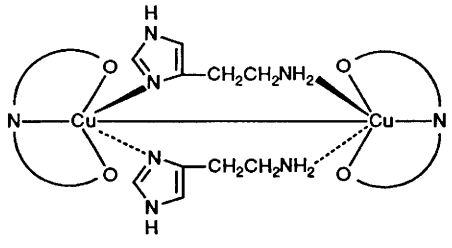

Interestingly, the histamine ligand does not bind in a bidentate mode to a single copper(II) ion but rather forms a bridge to a second copper(II) ion. Such a bridging mode has also been found[36] in the copper(I) complex [Cu_2(4-aeim)$_2$(CO)$_2$]-[BPh_4]$_2$.

Substitution of methyl or ethyl groups onto the imidazole ring structure therefore destroys the superexchange interaction producing monomeric units with a single unpaired electron. With 2-ethylamine a dipole–dipole coupled binuclear copper(II) complex is formed. The EPR spectra indicate that the above complexes possess a pseudo-C_3 axis of symmetry about each copper(II) ion which can only be accommodated by a five-co-ordinate system intermediate between a square pyramid and a trigonal bipyramid. Of interest is the similarity of the EPR spectra of the methyl and ethyl derivatives with that of superoxide dismutase (Fig. 11, Table 7). The latter has been shown by X-ray crystallographic studies to contain a copper(II) ion co-ordinated to four histidines (His-44, -46, -61, -118) and one water molecule, with the His-61 bridging copper(II) and zinc(II) ions.[28,37] Thus the five-co-ordinate geometry around the copper(II) ion is similar in both superoxide dismutase and the methyl and ethyl derivatives of the [Cu(pydca)L(H_2O)] complexes. Similar hyperfine and linewidth anisotropy are also observed for the superoxide dismutase and the methyl and ethyl derivatives. The small hyperfine coupling associated with g_2 is present as shoulders [Fig. 7(*b*)] in the spectrum of superoxide dismutase.[38] The increased magnitude of A_1 indicates that the metal-ion geometry is closer to a square pyramid than that of the complexes observed in the present study.

Conclusion

The co-ordination geometry of the copper centre in [Cu(pydca)L(H_2O)] complexes with L = 1-, 2- and 5-methylimidazole, can be described as intermediate between square pyramidal and trigonal bipyramidal. The intermediate nature between these two geometries has been characterised by Addison *et al.*[39] using the parameter $\tau = (\theta_1 - \theta_2)/60°$ where θ_1 and θ_2 are the two *trans* angles in the basal plane (τ = 0 for square pyramidal, 1 for trigonal bipyramidal). For complexes **1**–**3** the τ values are 0.30, 0.34 and 0.31 respectively. In the light of the large N(pydca)–Cu–N(Him) angles [172.1, 168.6 and 169.4°

in **1**–**3**] the co-ordination geometry around Cu^{II} in these complexes is closer to square pyramidal superimposed by a C_{2v} distortion. Nevertheless the intermediate nature between square planar and trigonal bipyramidal must be noted. The co-ordination symmetry is largely retained in going from the solid state to solution as evidenced by the electronic and EPR spectral data. The similar hyperfine and linewidth anisotropy observed for both superoxide dismutase and the methyl and ethyl derivatives of these [Cy(pydca)L(H_2O)] complexes warrants further work involving multifrequency EPR measurements of ^{63}Cu-enriched complexes. Such efforts are expected to lead to a better understanding of the electronic properties of these complexes, which in turn should allow for in-depth comparison to be made with those of superoxide dismutase.

References

1 H. Sigel and D. B. McCormick, *Acc. Chem. Res.*, 1970, **3**, 201.
2 H. Sigel, P. R. Huber, R. Griesser and B. Prijs, *Inorg. Chem.*, 1973, **12**, 1198.
3 H. Griesser and H. Sigel, *Inorg. Chem.*, 1970, **9**, 1238.
4 P. R. Huber, R. Griesser and H. Sigel, *Inorg. Chem.*, 1971, **10**, 945.
5 P. O. Brien, *J. Chem. Soc., Dalton Trans.*, 1981, 1540.
6 W. L. Kwik and K. P. Ang, *Aust. J. Chem.*, 1978, **31**, 459.
7 W. L. Kwik, K. P. Ang, H. S. O. Chan, V. Chebolu and S. K. Koch, *J. Chem. Soc., Dalton Trans.*, 1986, 2519.
8 W. Fitzgerald, J. Foley, D. McSweeney, N. Ray, D. Sheahan, S. Tyagr, B. J. Hathaway and P. O'Brien, *J. Chem. Soc., Dalton Trans.*, 1982, 1117.
9 G. M. Sheldrick, Siemens, Madison, WI.
10 R. W. Garret, unpublished work.
11 G. Dougherty, J. R. Pilbrow, A. Skorobogarty and T. D. Smith, *J. Chem. Soc., Faraday Trans. 2*, 1985, 1739.
12 T. E. Freeman, Ph.D. Thesis, Monash University, 1973.
13 W. C. Lin, *Mol. Phys.*, 1973, **25**, 247.
14 J. R. Pilbrow, *J. Magn. Reson.*, 1984, **58**, 186; *Transition Ion Electron Paramagnetic Resonance*, Clarendon Press, Oxford, 1990.
15 J. R. Pilbrow, *Mol. Phys.*, 1969, **16**, 307.
16 M. J. Nilges, Ph.D. Thesis, University of Illinois, Urbana, IL, 1979; R. L. Belford and M. J. Nilges, *Computer Simulation of Powder EPR Spectra*, EPR Symposium, 21st Rocky Mountain Conference, Denver, CO, 1979; G. R. Sinclair, Ph.D. Thesis, Monash University, 1989.
17 W. Froncisz and J. S. Hyde, *J. Chem. Phys.*, 1980, **73**, 3123; J. S. Hyde and W. Froncisz, *Annu. Rev. Biophys. Bioeng.*, 1982, **11**, 391.
18 G. R. Hanson, unpublished work.
19 R. A. Martinelli, G. R. Hanson, J. S. Thompson, B. Holmquist, J. R. Pilbrow and B. L. Vallee, *Biochemistry*, 1988, **28**, 2251.
20 T. D. Smith and J. R. Pilbrow, *Coord. Chem. Rev.*, 1974, **13**, 173.
21 M. Sato, S. Nagal, K. Ohmal, J. Nakaya, K. Miki and N. Kasai, *J. Chem. Soc., Dalton Trans.*, 1986, 1949.
22 H. C. Freeman, *Adv. Protein Chem.*, 1967, **22**, 257.
23 X. Solans, M. Aguilo, A. Gleizes, J. Faus, M. Julve and M. Verdaguer, *Inorg. Chem.*, 1990, **29**, 775.
24 M. L. Braden, E. W. Ainscough, E. N. Baker, A. M. Brodie and S. L. Ingham, *J. Chem. Soc., Dalton Trans.*, 1990, 2785.
25 L. T. Taylor and W. M. Coleman, *Inorg. Chim. Acta*, 1982, **63**, 183.
26 A. G. Bingham, H. Bogge, A. Muller, E. W. Ainscough and A. M. Brodie, *J. Chem. Soc., Dalton Trans.*, 1987, 493.
27 E. Bernarducci, W. F. Schwindinger, J. L. Hughay, W. K. Krogh-Jespersen and H. J. Schugar, *J. Am. Chem. Soc.*, 1981, **103**, 1686.
28 K. M. Beem, D. C. Richardson and K. V. Rajagopalan, *Biochemistry*, 1977, **16**, 1930.
29 F. Cariati, L. Erre, G. Micera, A. Panzanelli, G. Ciani and A. Sironi, *Inorg. Chim. Acta*, 1983, **80**, 57.
30 J. D. Dunitz, *Acta Crystallogr.*, 1957, **10**, 307.
31 W. Duffy, jun., J. E. Venneman, D. L. Strandberg and P. M. Richards, *Phys. Rev. B*, 1974, **9**, 2220.
32 R. C. Hughes, B. Morosin, P. M. Richards and W. Duffy, jun., *Phys. Rev. B*, 1975, **11**, 1795.
33 A. Bencini and D. Gatteschi, *Electron Paramagnetic Resonance of Exchange Coupled Systems*, Springer, Berlin, 1990.
34 G. R. Hanson, in preparation, 1991.
35 A. Bencini, I. Bertini, D. Gatteschi and A. Scozzafava, *Inorg. Chem.*, 1978, **17**, 3194.
36 M. Pasquali, D. Floriani, A. Gaetani-Manfredotti and C. Guastini, *J. Chem. Soc., Chem. Commun.*, 1979, 197.
37 J. A. Tainer, E. D. Getzoff, K. M. Beem, J. S. Richardson and D. C. Richardson, *J. Mol. Biol.*, 1982, **160**, 181.
38 E. M. Fielden and S. Rotilio, in *Copper Proteins and Copper Enzymes*, ed. R. Lontie, CRC Press, Boca Raton, FL, 1984, vol. 2, p. 27.
39 A. W. Addison, T. N. Rao, J. Reedijk, J. van Rija and G. C. Verschoor, *J. Chem. Soc., Dalton Trans.*, 1984, 1349.

Received 27*th March* 1991; *Paper* 1/01469B